Compendium of Earth and Space Sciences
ISSN Print: 3079-5621
ISSN Online: 3079-563X
https://doi.org/10.63313/CESS.4003

# Evolution of water cycle and its response to climate change

**Haihua An**
College of Resource and Environment, Henan Polytechnic University, Jiaozuo 454000, China

**How to cite this paper:** An, H. (2025). Evolution of water cycle and its response to climate change. Compendium of Earth and Space Sciences, 1(1), 32-49. ISSN Print: 3079-5621; ISSN Online: 3079-563X.
https://doi.org/10.63313/CESS.4003
**Published:2025-03-20**



## Abstract

The relationship between hydrological cycle and climate change is one of the most complex and key research topics in the earth science system. Under the background of global warming, ecological problems such as drought, flood and sea level rise occur frequently. In the face of rapid climate change, in-depth study of the geological evolution of the water cycle is of great significance for understanding the driving mechanism of climate change and predicting future climate trends. Based on this, this paper systematically discusses the influencing factors of water cycle and its interaction with climate change from a multi-faceted perspective. Temperature, vegetation growth and monsoon system have significant effects on water cycle at different scales. In order to quantitatively characterize the water cycle rate and its response to climate change, this paper summarizes a variety of climate-sensitive sediments and geochemical indicators that can record changes in the ancient water cycle. In addition, this paper also reviews two typical extreme climate events in the Earth 's history, the Paleocene-Eocene extreme heat event and the Late Paleozoic ice age, in order to explore the differences of water cycle under different climate backgrounds. Through the comparative analysis of the two events, this paper reveals that the water cycle response has spatial and temporal differences, and it is necessary to start a comprehensive exploration from multiple perspectives.

## Keywords

Water Cycle; Climate Sensitive Sediments; Geochemical Index; Extreme Climate; Space-Time Difference

## 1. Introduction

On the surface of the earth, water is the only molecule that can coexist in solid, liquid and gaseous states under natural conditions. The water cycle is mainly driven by solar radiation and earth stress [1], which promotes the evaporation of ocean water and surface water, and plants release water in gaseous form into the atmosphere through transpiration. Water vapor condenses under the action of atmospheric circulation and eventually returns to land and ocean in the form of rainfall and hail. At the same time, the water cycle between land and sea inputs precipitation into the ocean through surface runoff and underground reflux, forming the whole cycle of water on the earth ( Fig.1 ).

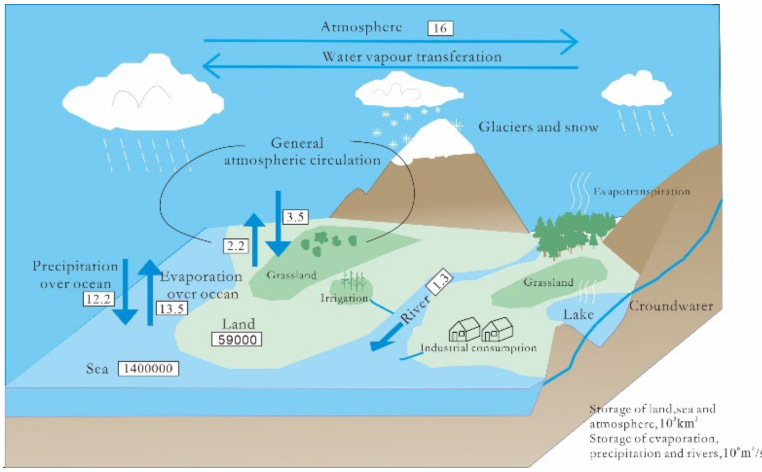


**Fig1:**Water cycle diagram (Storage data from Reference[2] )

The sixth assessment report of IPCC pointed out that the global temperature will rise by more than 1.5 °C in the future[3], and the sea level is expected to rise by 0.3 ~ 1.0 m by 2100[4] , and the precipitation pattern will also change. In the past half century, the global water cycle has responded significantly to climate warming, manifested as an increase in atmospheric water content [5], and an increase in the frequency of rainstorm and drought events[6,7]. The evolution of water cycle has become an urgent issue to cope with climate change. The modern earth system model takes the water cycle process and data as the core. The research shows that the changes of rainfall, evapotranspiration and surface runoff in China and the world 's major basins have shown spatial and temporal differences since 1979[8], and the water cycle is closely related to vegetation change[9] and human water use[10].For example, agricultural irrigation has aggravated the surface runoff and evapotranspiration rate[11]. However, due to insufficient understanding of the mechanism of the climate system, limited model resolution, and incomplete spatial and temporal coverage of data, the exact magnitude and spatial and temporal characteristics of the global water cycle response are still unclear. Therefore, the study of climate events and their ecological and environmental effects in geological history is of great significance for understanding the current global climate change.

The climate state in the geological history period is dynamically changing, often accompanied by a series of extreme climate events. Scholars at home and abroad have conducted extensive research on the geological evolution of the water cycle, such as the glacial sea-level changes in the Late Paleozoic Great Ice Age ( 360 ~ 260 Ma ) [12] and the extremely hot events at the turn of the Permian-Triassic [13]. During the entire water cycle, increased precipitation promotes terrestrial plant growth and organic carbon fixation, while enhancing continental silicate weathering. Terrestrial debris carries a large amount of nutrients into the ocean through surface runoff and other methods, which increases marine primary productivity and aggravates marine hypoxia and increases organic carbon burial. Therefore, the water cycle also affects the carbon cycle[14]. Changes in the amount of organic carbon burial regulate atmospheric PCO2 concentration, which in turn affects the global climate. Based on this, this paper introduces the controlling factors of water cycle and the climate-sensitive sediments and geochemical indexes indicating the rate of water cycle. By comparing the two extreme climates of the Paleocene-Eocene thermal event and the late Paleozoic ice age, the differences of water cycle in different climatic environments are discussed, which provides a scientific basis for predicting the future climate change trend.

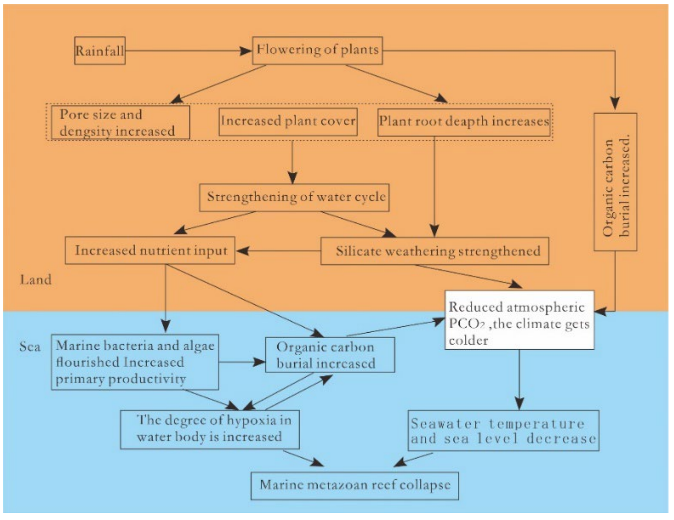


**Fig2:**Frame diagram of the relationship between plant, hydrological cycle and carbon cycle evolution ( modified from [15])

## 2 .Control factors of water cycle

### 2.1. Vegetation

The origin and prosperity of Paleozoic terrestrial plants have significantly changed the hydrological cycle. On the one hand, plants increase rainfall through transpiration, which promotes silicate weathering and organic carbon burial ; on the other hand, the release of humic acid from plant roots accelerates chemical weathering and inputs nutrients into the ocean through runoff, which promotes the increase of marine primary productivity, marine hypoxia and organic carbon burial [16]. The intensity of hydrological cycle is closely related to the structure of plants and the coverage area of vegetation. The deepening of vegetation roots enhances the absorption of soil and groundwater, promotes transpiration, and promotes the expansion of plants from humid lowlands to arid highlands, thereby strengthening the terrestrial hydrological cycle and increasing precipitation and runoff [17]. The increase of stomatal size and density also increases transpiration rate and affects hydrological cycle, while leaf size mainly reflects precipitation [18]. In addition, the vegetation coverage area also effectively coordinates the water cycle, especially dense forests. The root system of forest vegetation is deep and extends widely, which enhances soil permeability and is conducive to the supplement of precipitation to deep soil and groundwater. Canopy and litter layer can intercept and store part of the precipitation, reduce surface runoff and soil erosion [19]. Climate models show that small-scale deforestation may increase regional precipitation, but large-scale tropical deforestation can lead to soil erosion and bedrock exposure, reducing surface water storage capacity, leading to drought [20], and changing river flows and river patterns [21].

### 2.2. Temperature

The relationship between hydrological cycle and temperature is very complex. It is generally believed that the increase of temperature will aggravate the hydrological cycle. High temperature increases the capacity of atmospheric water vapor[22], resulting in a rapid increase in tropospheric water vapor. However, due to the limitation of radiation flux changes, the growth rate of global precipitation is lower than that of water vapor, thus slowing down the atmospheric circulation. According to the Clapeyron-Clausius ( c-c ) expression, in theory, the saturated water vapor pressure increases with the increase of temperature, and global warming increases the atmospheric water vapor content[8], which in turn affects the global water cycle. The climate model shows that the change of atmospheric water vapor content basically follows the c-c equation with the increase of temperature : for every 1 °C increase in temperature, the water vapor content increases by about 7 % [23]. However, the precipitation model is complex and strongly dependent on geographical location and climatic zones. The response of the water cycle to climate is not globally uniform, and the wet zone precipitation variability is more significant[24].

### 2.3. Astronomical orbit

In the geological history period, the Earth 's orbital periodic signals (precession, slope, eccentricity ) provide a key basis for explaining orbital-scale climate change. The study of water cycle on the orbital scale has become an important window to understand the global water cycle. Affected by the three elements of the orbit, there are differences in the changes of sea ice and precipitation in the northern and southern hemispheres of the Earth on the orbital scale : the sea ice in the northern hemisphere is controlled by the precession, the sea ice in the southern hemisphere is controlled by the slope, and the summer precipitation in northern China is mainly controlled by solar radiation and precession signals[25]. Similarly, there is the summer monsoon precipitation in the Sea of Japan[26]. Based on the general circulation model, Lawrence found that the response of the Eocene terrestrial climate to the precession was characterized by changes in precipitation or net evaporation, and the precipitation difference between the minimum and maximum precession was less than 10 %[27]. During the PETM period, due to the maximum amount of summer sunshine in the north, the eccentricity orbit suppresses extreme precipitation events in the eastern Atlantic and amplifies extreme precipitation events in the western Atlantic[28]. In addition, the enhanced orbital forcing makes the North American interior drier and the Asian interior wetter [29], and the paleosol cycle of the willwood Formation in the Bighorn Basin of the United States is related to the 21ky precession cycle [30].

### 2.4. Monsoon

Monsoon climate change is driven by external and internal forces, mainly characterized by changes in circulation and precipitation. Monsoon anomalies may trigger extreme weather events such as droughts and floods[31]. The global monsoon includes the global tropical and subtropical monsoons on the surface, and the global tropospheric and stratospheric monsoons in the vertical direction[32]. The Late Cretaceous-Paleogene South China was controlled by the westerly circulation system, and the water vapor input mainly came from the Tethys Ocean on the west side of the continent, which led to the regional drought away from the water vapor source in Huichang and Jitai Basins in Jiangxi Province, and the first deposition of anhydrite deposits[33], while the Lanping-Simao Basin deposited thick potassium salt deposits due to the subtropical high-pressure downdraft. After the Late Cretaceous, the northward movement of the Indian plate and the African plate, and the uplift of the Qinghai-Tibet Plateau caused by the collision of the Indo-European plate in the Late Paleocene, weakened the water vapor transport from the westerly circulation to South China, resulting in the expansion of the distribution range of the evaporite. With the uplift of the Tibetan Plateau to a certain height in the late Oligocene, the East Asian monsoon circulation system gradually formed, and the precipitation in South China and North China increased significantly.

## 3. Restoration of deep paleoclimatic indicators

### 3.1. Climate sensitive sediments

#### 3.1.1. Coal

Coal is in a humid climate environment, a large number of terrestrial woody plants flourished and gathered into peat, and finally formed after metamorphism, so it can be used as a qualitative index of humid environment in deep climate research. The formation of peat by plants is related to biochemical processes, which require a stable water environment to prevent the accumulation of organic matter from drying and oxidation. Therefore, almost all peat is accumulated in a humid basin environment characterized by high groundwater levels, and precipitation is usually > 100 cm yr-1, and precipitation exceeds evapotranspiration at least 10 months in a year [34]. Peat can be formed anywhere and at any time that meets these conditions. The results of geological records and climate simulation show that before 250 Ma, the median temperature of coal formation was 25 °C and the precipitation was 1300 mm yr-1. After 250 Ma, there were coal records with temperature between 0-21 °C and precipitation of 900 mm yr-1.The main distribution latitude of coal also shifted from warm and humid equatorial and low latitudes to rainy areas in the middle and high latitudes, with latitudes ranging from 23 ° to 58 °[35].

### 3.1.2. Evaporite

Evaporite is a kind of salt-bearing rock that is chemically precipitated from brine by evaporation. It can be divided into carbonate type, sulfate type, chloride type and mixed evaporite type according to lithofacies. Its sedimentary environment can be subdivided into Sabkha, supratidal zone, intertidal zone-subtidal zone and semi-deep sea-deep sea environment according to marine and continental facies, as well as intracontinental Sabkha, lakeshore, shallow lake and semi-deep lake-deep lake [36]. Evaporite is produced under the specific climatic conditions of high annual average temperature and low precipitation. Generally, the annual average precipitation is less than 1400 mm, and the months with precipitation greater than 1400 mm do not exceed 3 months, and the annual average temperature exceeds 15 °C[37]. The geological records of all Phanerozoic evaporites indicate that they almost always appear in the subtropical arid zones of the two hemispheres, and are now mainly formed in a narrow ( 25-40 ° ) latitude zone [38].

Some scholars also believe that evaporite is not only the product of strong evaporation under dry climate conditions, but also can be caused by the supersaturation of brine in deep water environment[39]. The Late Miocene saline lakes in Spain were frequently subjected to Mediterranean transgression, and the evaporite sequence is dominated by thick gypsum, glauberite and halite[40]. At present, as the only marine solid potash producing area in China, the low S isotope of the lower Carboniferous evaporite in the Simao Basin shows that in addition to volcanic hydrothermal recharge, the transgression during the Middle Tethys is also an important recharge form [41]. In addition, some scholars believe that evaporites may be affected by geothermal action, especially ancient thick evaporites. Many ancient evaporite formations often appear on a large scale in a certain area, with a large area and thickness, and a short time span. The classical view of evaporation caused by solar energy cannot explain this phenomenon. For example, the currently discovered Mediterranean-Red Sea, Mexico-South Atlantic and other deep-sea mega-thick evaporites are even more challenging to the sun [42].

### 3.1.3. Bauxite

Bauxite is a chemical residue produced by strong onshore weathering under hot and humid climate conditions. It is composed of alumina or hydroxide and contains a small amount of hydroxyl iron oxide and clay minerals [43].Therefore, bauxite is usually regarded as a climate-sensitive sediment indicating hot and humid climate conditions [44]. For example, after the Middle Devonian, vegetation flourished, and plants strengthened the water cycle and deposited high-abundance bauxite abundance, indicating a warmer and wetter global climate[45]. The formation of bauxite requires the combined action of climate, structure, hydrology, geography and geomorphology, vegetation coverage and atmospheric composition. According to its formation characteristics, it can be divided into laterite type, sedimentary type and karst type[46]. The process of laterization is most active in tropical regions with an annual average temperature of not less than 20 ° C and a humidity of more than 1200 mm yr-1. Sedimentary bauxite deposits are mainly formed by the mechanical erosion of surface water flow and debris accumulation on plateau slopes and foothills, which characterizes the hydrodynamic degree of solution filtration rate. Due to the accumulation space and good drainage system provided by karst dissolution, karst terrain is a favorable environment for bauxite accumulation. Many modern bauxite strata, such as western Guangxi, southern China and northern Vietnam, are formed on karst terrain [47]. The size of bauxite deposits depends on temperature and humidity conditions. Generally speaking, large bauxite deposits are mainly concentrated in coastal areas, and their humidity is usually higher than that in the mainland. Combined with the existing climate model, distribution and atmospheric circulation model results of bauxite formation, scholars believe that the climatic conditions of annual average temperature > 22 ° C, annual average precipitation > 1200 mm, precipitation 23 ° C, and precipitation greater than evaporation for at least 6 months per year are more conducive to the formation of bauxite [48]. It is generally formed in a terrestrial environment or a sea-land transition environment [45].

#### 3.1.4. Red layer

The red layer is a kind of continental clastic rock sedimentary strata with red as the main color, which is formed by the weathering and denudation of the original bedrock under certain temperature and heat conditions and the sedimentary consolidation and diagenesis in the ancient basin or lake basin. According to the different formation environment, it can be divided into oceanic red layer and continental red layer. The rock types of oceanic red beds mainly include limestone, marl, calcareous shale, mudstone, shale and siliceous rocks. The sedimentary environment is dominated by continental slopes and deep-water basins, while the lithology of continental red beds is more complex, covering conglomerate to mudstone. Rocks of various sizes, and may be sandwiched with freshwater limestone, gypsum and rock salt layers[49]. Red beds are widely distributed in China, first appeared in the Carboniferous, widely distributed in the Tertiary. Because the red layer is often mixed with gypsum layer, and the red color of the red layer mainly comes from the oxidation of iron ions in minerals, most scholars believe that the continental red layer indicates the arid and hot climate environment[49]. However, at the same time, the formation of the red layer must have the relative enrichment of trivalent iron, and this process requires sufficient leaching and has a strong seasonality [39,50].Therefore, the paleoenvironment formed by the red layer is not completely dry and hot, and may also be formed in a semi-arid and semi-humid climate.

#### 3.1.5. Clay minerals

For clay minerals, illite is usually produced by aluminosilicate minerals such as feldspar and mica under the condition of weathering and de-K +.Illite is mostly formed in arid and cold weak leaching and weak alkaline environment, which generally reflects the dry climate[51]. For example, under the hot and humid climate conditions, the development of wetland vegetation makes the surface water acidic, and the aluminosilicate minerals in the parent rock will be further decomposed into kaolinite by strong leaching[52,53]. Although the warm and humid climate is conducive to the formation of kaolinite, the climate information of kaolinite can be preserved only when the climate turns dry. Therefore, only the detrital kaolinite formed and preserved by in-situ weathering reflects the hot and humid climate. Chlorite is mainly derived from low-grade metamorphic rocks and ferruginous rocks. It is formed in an alkaline environment where chemical weathering is inhibited and weak leaching. The increase in its content generally means that the climate gradually becomes arid [54].

However, only those clay minerals that have not undergone post-diagenetic changes can truly reflect the weathering and climatic conditions in the source area and the basin. Due to the influence of high temperature and high rainfall, the strong hydrolysis of minerals leads to poor crystallinity. On the contrary, the crystallization of minerals is preserved under low temperature and dry climate conditions[55]. Therefore, we can also use the degree of crystallization of minerals to judge the climate of the source area. For example, the illite crystallinity index is 1 nm half-peak width. The low value indicates that the illite crystallinity is high, reflecting the dry and cold climate, and the high value indicates that the crystallinity is poor, reflecting the warm and humid climate.

### 3.2. Geochemical index

#### 3.2.1. Sr / Ba

The exchange of fresh water between the atmosphere and the ocean is coordinated with the mixing of the ocean circulation, which enhances the sensitivity of salinity to the evaporation-precipitation balance[56]. Precipitation and runoff input fresh water to the ocean, diluting surface salinity, while evaporation increases salinity. The Sr / Ba ratio can not only effectively indicate paleosalinity[57], but also reflect the water cycle of sedimentary environment [58]. Sr is more mobile and soluble than Ba, and is easy to migrate to the marine environment with precipitation and groundwater. With the continuous enhancement of seawater evaporation and the increase of salinity, $Sr^{2+}$ can replace $K^+$ and $Ca^{2+}$ in the rock lattice, while $Ba^{2+}$ can combine with sulfate ions to form barium sulfate precipitation under the neutralization of limestone, resulting in Sr element is more enriched than Ba element. Therefore, the Sr / Ba ratio can also indicate precipitation and water cycle intensity. The lower the ratio, the stronger the leaching effect, the increase of precipitation and the enhancement of water cycle[59].

#### 3.2.2. Oxygen isotopes

The oxygen isotope value as a marine thermometer can sensitively reflect the water cycle processes such as evaporation, condensation, and precipitation, so oxygen isotope is considered to be an effective means to study the hydrological cycle process. The $\delta^{18}O$ value of the seawater is controlled by hydrological conditions such as evaporation intensity, freshwater injection and high-latitude glaciers. Due to the high saturated water vapor pressure of heavy isotope water molecules, under the same temperature conditions, light isotope water molecules are more likely to break free from molecular gravity and enter the air than isotope water molecules, so that the remaining water body enriches heavy isotopes and evaporates water vapor to enrich light isotopes, that is, isotope fractionation effect. Therefore, evaporation will preferentially take away $^{16}O$ in seawater, resulting in $^{18}O$ enrichment in seawater. The injection of a large amount of external water will reduce the $\delta^{18}O$ value in seawater. At the same time, due to the transfer of water vapor from low latitudes to high latitudes, the condensed rainfall process selectively deposits $^{18}O$-enriched water vapor, resulting in a significant loss of $\delta^{18}O$ values in high-latitude river water and glaciers[60]. Because most of the fresh water stored in glaciers is derived from rainfall at high latitudes and high altitudes where $^{18}O$ is extremely depleted, large-scale glacier development will increase the $\delta^{18}O$ value of seawater, and glacier ablation will cause the $\delta^{18}O$ value of seawater to decrease[61]. In general, high evaporation intensity results in relatively high salinity and oxygen isotope values in surface seawater in arid areas, while near river estuaries or high-latitude oceans, salinity and oxygen isotope values are relatively low due to large amounts of freshwater input[60].

### 3.3. Biomarkers

#### 3.3.1. Lipid compounds

Sedimentary lipid compounds are widely used to reconstruct paleohydrological climate changes, such as long-chain n-alkanes of higher plants and microbial hopanes, short-chain iso-fatty alcohols and tetraether membrane lipids ( GDGTs ) [62-64]. As the main component of plant leaf wax, long-chain n-alkanes can be preserved in geological bodies for a long time due to their special structure and are not easily degraded by microorganisms. The study confirmed that the average carbon chain length ( ACL ) of n-alkanes is inversely proportional to latitude. In low latitude areas, the temperature is high and the evaporation is strong. Plants synthesize longer carbon chain compounds to reduce water loss. At high latitudes, shorter carbon chain compounds are synthesized. The carbon-containing advantage index ( CPI ) reflects the climate state in peat deposition. The high CPI value indicates cold and dry climate, and the low CPI value indicates warm and humid climate. Sun et al.used the ratio of aquatic plant communities to total plant communities ( PAQ ), ACL, CPI and other parameters to reconstruct the paleohydrological changes in the middle and late Holocene of the Loess Plateau, and found that the climate in this area was humid in the middle Holocene, which was contrary to the record in central China[65]. In addition, the carbon isotope ( $\delta 13C$ ) of leaf wax n-alkanes can also characterize the hydrological climate. Liu et al.found that the $\delta 13C$ of C3 plants was significantly negatively correlated with the annual mean precipitation ( MAP ), while the $\delta 13C$ of C4 plants was not significantly correlated with MAP[66].Therefore, the $\delta 13C$ of C3 plants is more suitable for the reconstruction of ancient precipitation, while C4 is suitable for the reconstruction of ancient temperature.

### 3.3.2. Pollen

Because of its long-term preservation in the ground and strong stability, spore-pollen can reflect the type of plant mother, and then indicate the climate and environmental information of the basin. Scholars divided the sporopollen vegetation types into coniferous trees, evergreen broad-leaved trees, deciduous broad-leaved trees, shrubs and herbs, and divided the sporopollen climate types into tropical, subtropical, temperate and temperate tropical-subtropical, tropical-temperate plants. According to the dry and wet degree of pollen, it is divided into xerophytic, mesophytic, hygrophytic, aquatic and marshy[67,68]. Sporopollen assemblage and proportion analysis showed that coniferous plants such as spruce and fir indicated cold and dry environment. The increase in the number of Artemisia, Compositae, and Chenopodium pollen in herbaceous plants represents a dry and dry climate, while Gramineae herbaceous plants reflect humid conditions [69] ; the increase of ferns usually indicates humid climate or sea level rise [70]. For example, the climate change reflected by the Quaternary sporopollen assemblage in Hengsha Island, Shanghai is consistent with the global climate change trend. The climate is dry and cool during the glacial period, and the climate becomes warm and wet during the interglacial period [69]. A large number of Artemisia and Chenopodium pollens found in the Hulun Lake area during the Holocene represent the arid and less rainy climate ; less grasses indicate an increase in short-term precipitation [71]. The Late Pleistocene sporopollen records in the Qingshuihe Basin, Ningxia, China, show that the vegetation changed from dry grassland represented by Artemisia to desert grassland, and the climate changed from cool and humid to cold and dry, reflecting the enhancement of the winter monsoon[72].

## 4. Evolution of water cycle in geological period

### 4.1. Paleocene-Eocene thermal events

The Paleocene-Eocene Polar Thermal Event ( PETM, ~ 56 Ma ) is a sudden extreme warming event in the Cenozoic, with a total duration of about 200 kyr[73], accompanied by negative carbon isotope shift ( CIE ) [74], ocean acidification [75] and accelerated deposition rate[76]. The data simulation shows that the increase of $CO_2$ level during PETM leads to the overall increase of global precipitation, and the precipitation in tropical and high latitudes increases significantly, while the precipitation in subtropical regions decreases, and the precipitation intensity in the Northern Hemisphere has seasonal variation[28]. The increase in freshwater runoff promotes nutrient input and increases primary productivity, which may be related to the abundance of Apectodinium[76]. Authigenic carbonate geochemical indicators molar Mg / Ca and Sr / Ca ratios indicate an overall increase in precipitation throughout the PETM, consistent with the disappearance of dolomite and the presence of kaolinite in the strata[77]. In terrestrial systems, changes in the morphology of river systems also respond to increases in rainfall and sediment deposition[78]. Osmium isotopes and hydrogen isotopes of plant leaf wax further confirm that the hydrological cycle is accelerated [79,80]. However, the humid climate during the PETM period is not universal, and some regions have experienced severe droughts. Paleosol and carbonate nodule analysis in the Bighorn Basin, Wyoming, USA shows that the region experienced a transition from dry to humid climate patterns, which may be related to the precession cycle[81]. In East Africa, although biomarker concentrations increased in the early stages of PETM, plant leaf wax n-alkanes ( C27, C29 and C31 ) were deuterium-rich, indicating a hot and arid climate[82]. Mineralogical studies in northern Spain have shown that the climate transitioned from arid to semi-arid, accompanied by extensive evaporite deposition[83].

At present, the trigger mechanism of PETM event is not clear. Most scholars believe that the occurrence of PETM event is due to the rapid release of huge amount of light carbon into the ocean and atmosphere. The acidification of seawater caused by light carbon leads to the dissolution of $CaCO_3$ in the deep sea environment, resulting in the reduction of organic carbon burial [84]. Another view is that PRTM is related to orbital forcing. Astronomical calculations show that the PETM burst began near the maximum eccentricity [85]. Orbital forcing destroys the unstable carbon sources of land and ocean through the feedback mechanism of ocean and atmospheric circulation, triggering the PETM event [28].

### 4.2. Late Paleozoic glacial period

The Late Paleozoic Ice Age ( LPIA ) began in the Late Devonian, and reached its peak from the late Carboniferous to the early Permian after a significant expansion. It is the longest glacial event since the Phanerozoic[12]. The glacial period has experienced many short glacial and warm period alternations, namely the so-called glacial-interglacial period[86]. When the amount of global glaciers changes, the sea level also changes. During the glacial period, the climate temperature was low, a large amount of $H_2O$ existed in the form of glaciers, and the global sea level decreased. During the interglacial period, the warming climate led to the melting of glaciers and the rise of sea level [87]. These changes cause fluctuations in the global climate and are recorded by indirect substitutes of marine and continental sediments in the mid-low latitudes, such as extensive cyclostratigraphy, biota turnover[88,89], positive carbon isotope shift [90], and positive conodont δ18O shift [91]. Due to the different development degrees of the late Paleozoic glacial period, glacial diagenesis is widely distributed in the middle and high latitudes of the Southern Hemisphere.As the range of glaciers expands from the late Carboniferous to the early Permian, glacial diagenesis began to form in Australia in the middle and low latitudes. The stratigraphic and sedimentary data show that the late Paleozoic glacial period experienced at least eight discrete glacial periods[92].

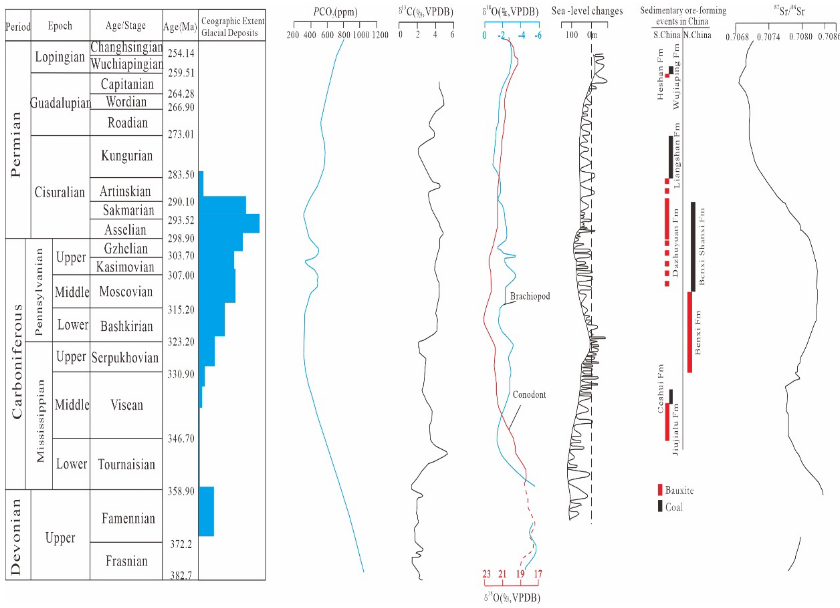


**Fig3:**Late Paleozoic glacial deposits, paleo-carbon dioxide and environmental change geochemical proxy map

Late Paleozoic glacial deposits from[93] ; the paleo-carbon dioxide and geochemical proxies were modified from[94] ; the sea level change is cited from [95] ; the sedimentary mineralization events in China are cited from [96].

During the LPIA, although the global average annual rainfall is relatively stable, the spatial and temporal distribution is extremely uneven. The study of paleosol, evaporite, flora and sedimentology in the western Tethys and central European continent reveals the seasonal climate of semi-humid-semi-arid-arid from the late Visean glaciers to the Shepkhovian, and then to the early Permian glacier retreat [97].In the low latitudes, the water cycle is affected by the tropical convergence zone. The expansion and decay of the high-latitude Gondwana ice sheet significantly affect the low-latitude hydrological cycle and climate by affecting the migration of the tropical convergence zone ( ITCZ ) of the atmospheric circulation. The expansion of the

Gondwana continental ice sheet caused the ITCZ to shrink to the vicinity of the equator, resulting in the formation of a humid climate zone in the Pangu continent and an increase in annual rainfall. In the interglacial period, the decrease of ice volume leads to the decrease of polar high pressure, the expansion of ITCZ zone and the decrease of annual rainfall in the tropics [98]. From the late Carboniferous to the early Permian, the low-latitude North China plate showed a relatively cool and humid and warm and humid climate model in the glacial and non-glacial periods, respectively. The presence of kaolinite is consistent with the glacial and non-glacial succession in the high-latitude Gondwana region [99] . The sudden increase in the inflow of siliceous debris in the relatively stable carbonate-siliceous clastic rock sequence in the southeastern part of the South China block in the paleotropics is considered to be caused by the enhancement of precipitation events related to the periodic occurrence of glacier-interglacial periods [100], reflecting the enhancement of the water cycle in the paleotropics. The extensive deposition of bauxite also means that the eastern part of the Tethys is a climate model with high annual humidity and seasonal dryness[101].

## 5.Conclusions

Global climate change is expected to further aggravate the water cycle, resulting in accelerated evaporation and increased precipitation, and water cycle sensitivity will become a key issue for decades. In this paper, the effects of temperature, vegetation, astronomical orbit and monsoon on the water cycle are reviewed. Combined with climate-sensitive sediments, geochemical parameters and biomarkers, the response of the late Paleozoic glacial and Paleocene-Eocene extreme heat events to the water cycle is discussed. Studies have shown that climate warming usually aggravates the water cycle, while climate cooling weakens the water cycle. However, the spatial distribution of hydrological climate change is uneven, and the variability at regional, continental and global scales is difficult to quantify. Therefore, further research is needed to provide new insights into current and future hydrological climate change.

## References

[1] Oki T, Kanae S J S. Global hydrological cycles and world water resources[J], 2006, 313(5790): 1068-1072.

[2] Song Hanchen, Song Haijun, Zhang Zhongshi, et al. Evolution and driving mechanism of water cycle at the intersection of Paleozoic and Mesozoic. Chinese Science Bulletin[J], 2023, 68(12): 1501-1516.

[3] Masson-Delmotte V, Zhai P, Pirani S, et al. Ipcc, 2021: Summary for policymakers. in: Climate change 2021: The physical science basis. contribution of working group i to the sixth assessment report of the intergovernmental panel on climate change[J], 2021.

[4] Li Mingsong, Zhang Haotian, Wang Meng, et al. Astronomically driven groundwater reservoirs and sea level changes during the greenhouse period. Chinese Science Bulletin[J], 2023, 68(12): 1517-1527.

[5] Yu L, Josey S A, Bingham F M, et al. Intensification of the global water cycle and evidence from ocean salinity: a synthesis review[J], 2020.

[6] Extremes P J N. Atmospheric Warming and the Amplification of[J], 2008, 454: 204.

[7] Allan R P, Soden B J J S. Atmospheric warming and the amplification of precipitation extremes[J], 2008, 321(5895): 1481-1484.

[8] Su Buda, Sun Hermione, Li Xiucang, et al. Temporal and spatial evolution of China's land water cycle in the context of climate change. Journal of Atmospheric Sciences, 2020, 43(06): 1096-1105.

[9] Bonan G B J S. Forests and climate change: forcings, feedbacks, and the climate benefits of forests[J], 2008, 320(5882): 1444-1449.

[10] Zhang J. Impact of damming interception on water cycle in Wujiang River Basin[D]. 2018.

[11] Lv Meixia, Ma Zhuguo, Li Mingxing. Research progress on climate change, vegetation change, human water use and water cycle in the Yellow River Basin. Journal of Atmospheric Sciences [J]: 1-14.

[12] Zhong Yutian, Chen Jitao, Gao Biao, et al. Review and prospect of carbon-water cycle in Late Paleozoic Great Ice Age. Chinese Science Bulletin[J], 2023, 68(12): 1544-1556.

[13] A W Q W, B C G, A F F Z, et al. A high-resolution Middle to Late Permian paleotemperature curve reconstructed using oxygen isotopes of well-preserved brachiopod shells[J], 540.

[14] Guo Xuning, Li Yunling, Yan Jiaming, et al. Response to sewage cycle and changes in water demand under the "two-carbon" strategy. South-to-north Water diversion and Water Science and Technology [J], 2023, 21(01): 22-28+38.

[15] Yao Le, Huang Pu, Chen Bo. Coupling evolution of plant water cycle and reef in the Late Devonian-Mississippian Subera. Chinese Science Bulletin[J], 2023, 68(12): 1473-1486.

[16] Algeo T, Berner R, Maynard J, et al. Late Devonian oceanic events and biotic crises: 'rooted' in the evolution of vascular land plants[J], 1995.

[17] Boyce C K, Lee J E J a R O E, Sciences P. Plant Evolution and Climate Over Geological Timescales[J], 2016, 45(1): annurev-earth-063016-015629.

[18] Wilf P, Wing S L, Greenwood D R, et al. Using fossil leaves as paleoprecipitation indicators: an Eocene example[J], 1998, 26(3): 203-206.

[19] Xiao Y. Water conservation function of forest ecosystem and its measurement method. Chinese Journal of Ecology[J], 2009, 28(03): 529-534.

[20] Xu G, Shen J, Algeo T J, et al. Limited change in silicate chemical weathering intensity during the Permian–Triassic transition indicates ineffective climate regulation by weathering feedbacks[J], 2023, 616: 118235.

[21] Benton M J, Newell A J J G R. Impacts of global warming on Permo-Triassic terrestrial ecosystems[J], 2014, 25(4): 1308-1337.

[22] Soden B. Robust Responses of the Hydrological Cycle to Global Warming[C]. AGU Fall Meeting Abstracts, 2008: H13H-05.

[23] Held I M, Soden B J J J O C. Robust Responses of the Hydrological Cycle to Global Warming[J], 2006, 19: 5686-5699.

[24] Pratap S, Markonis Y J P I E, Science P. The response of the hydrological cycle to temperature changes in recent and distant climatic history[J], 2022, 9(1): 1-37.

[25] Wu Zhipeng, Yin Qiuzhen, Liang Mingqiang, et al. Characteristics of influence of orbit drive on water cycle at high and low latitudes: sea ice and precipitation. Chinese Science Bulletin[J], 2023, 68(12): 1443-1458.

[26] Hayashi R, Sagawa T, Irino T, et al. Orbital-scale vegetation-ocean-atmosphere linkages in western Japan during the last 550 ka based on a pollen record from the IODP site U1427 in the Japan Sea[J], 2021, 267: 107103-.

[27] Lawrence K T, Sloan L C, Sewall J. Terrestrial climatic response to precessional orbital forcing in the Eocene[J], 2003.

[28] Rush W D, Kiehl J T, Shields C A, et al. Increased frequency of extreme precipitation

events in the North Atlantic during the PETM: Observations and theory[J], 2021, 568: 110289.

[29] Kiehl, Jeffrey, T., et al. Greenhouse- and orbital-forced climate extremes during the early Eocene[J], 2018.

[30] Aziz H A, Hilgen F J, Luijk G M V, et al. Astronomical climate control on paleosol stacking patterns in the upper Paleocene–lower Eocene Willwood Formation, Bighorn Basin, Wyoming[J], 2008, 36(7): 531-534.

[31] Zhisheng A, Guoxiong W, Jianping L, et al. Global monsoon dynamics and climate change[J], 2015, 43(1): 29-77.

[32] Pinxian W J. Global monsoon in a geological perspective[J], 2009, 054(007): 1113-1136.

[33] Wang Jiuyi, Liu Chenglin, Wang Chunlian, et al. Coupling structural and climatic control of evaporite deposit formation in South China from Late Cretaceous to Paleogene. Acta Geologica Sinica[J], 2021, 95(07): 2041-2051.

[34] Cecil C B, Stanton R W, Neuzil S G, et al. Paleoclimate Controls on Late Paleozoic Sedimentation and Peat Formation in the Central Appalachian Basin (USA)[J], 1985, 5(1): 195-230.

[35] Bao X, Hu Y, Scotese C R, et al. Quantifying climate conditions for the formation of coals and evaporites[J]. National Science Review, 2023, 10(6).

[36] Zhong Yisi, Wang Licheng, Dong Haowei. Evaporite sedimentary characteristics and environment review. Acta Sedimentologica Sinica[J], 2022, 40(05): 1188-1214.

[37] Craggs H J, Valdes P J, Widdowson M J P, Palaeoclimatology, Palaeoecology. Climate model predictions for the latest Cretaceous: an evaluation using climatically sensitive sediments as proxy indicators[J], 2012, 315: 12-23.

[38] Warren J K J E-S R. Evaporites through time: Tectonic, climatic and eustatic controls in marine and nonmarine deposits[J], 2010, 98(3-4): 217-268.

[39] Tian Xin, Xiang Fang, Luo Lai, et al. Research methods and climatic significance of special continental sediments. Earth Science Frontiers [J], 2009, 16(05): 71-78.

[40] Salvany J M, GarcÍa-Veigas J, Sedimentology F O J. Glauberite–halite association of the Zaragoza Gypsum Formation (Lower Miocene, Ebro Basin, NE Spain)[J], 2007.

[41] Miao Zhongying, Zheng Mianping, Zhang Xuefei, et al. Sulfur isotope geochemistry of Lower Cretaceous evaporite in Simao Basin and its significance for potassium salt mineralization. Journal of Earth Science[J], 2019, 40(02): 279-290.

[42] Qin Z, Tang C, Zhang X, et al. Large Evaporite Provinces: Geothermal rather than Solar Origin?[J], 2020.

[43] Retallack G J J E G. Lateritization and bauxitization events[J], 2010, 105(3): 655-667.

[44] Du Yuansheng, Yu Wenchao. Continental leaching mineralization of sedimentary bauxite: a discussion on genetic classification of bauxite deposits. Journal of Palaeogeography [J], 2020, 22(05): 812-826.

[45] Geology G B J D I E. Karst bauxites. Bauxite deposits on carbonate rock[J], 1982, 14: 1-441.

[46] Bogatyrev B A, Zhukov V V, Tsekhovsky Y G J L, et al. Formation conditions and regularities of the distribution of large and superlarge bauxite deposits[J], 2009, 44(2): 135-151.

[47] Yu W, Wang R, Zhang Q, et al. Mineralogical and geochemical evolution of the Fusui bauxite deposit in Guangxi, South China: From the original Permian orebody to a Quarternary Salento-type deposit[J], 2014, 146: 75-88.

[48] Gregory, D., Price, et al. Prediction of modern bauxite occurrence: implications for climate reconstruction[J], 1997, 131(1-2): 1-13.

[49] Wang Chengshan, Hu Xiumian. Cretaceous world and magenta beds. Earth Science Frontiers [J], 2005(02): 11-21.

[50] Wang C, Hu X, Sarti M, et al. Upper Cretaceous oceanic red beds in southern Tibet: a major change from anoxic to oxic, deep-sea environments[J], 2005, 26(1): 21-32.

[51] Galán E, Ferrell R E J D I C E. Genesis of Clay Minerals[J], 2013, 5: 83-126.

[52] Garzanti E, Padoan M, Setti M, et al. Provenance versus weathering control on the composition of tropical river mud (southern Africa)[J], 2014.

[53] Dinis P A, Garzanti E, Hahn A, et al. Weathering indices as climate proxies. A step forward based on Congo and SW African river muds[J], 2020(201-): 201.

[54] Gingele F X, Deckker P D, Hillenbrand C D J J O T G S O A. Late Quaternary fluctuations of the Leeuwin Current and palaeoclimates on the adjacent land masses: clay mineral evidence[J], 2001, 48(6): 867-874.

[55] Winkler A, Wolf-Welling T, Stattegger K, et al. Clay mineral sedimentation in high northern latitude deep-sea basins since the Middle Miocene (ODP Leg 151, NAAG)[J], 2002, 91(1): 133-148.

[56] Wetzel R G. Limnology: Lake and River Ecosystems[M]. Limnology: Lake and River Ecosystems, 2001.

[57] Qiang Lei. Geochemical characteristics of the Ordovician rocks in the southwest margin of Ordos and its paleo-oceanic paleoclimate significance [D]. 2019.

[58] Wei W, Algeo T J J G E C A. Elemental proxies for paleosalinity analysis of ancient shales and mudrocks[J], 2020, 287: 341-366.

[59] Meng Zhongneng. Common paleoclimate research methods and prospects. Journal of Guizhou Institute of Engineering Application Technology [J], 2021, 39(03): 56-60.

[60] Chen Bo, Zhu Maoyan. Application of oxygen isotope in paleotemperature reconstruction and water cycle research. Chinese Science Bulletin[J], 2023, 68(12): 1528-1543.

[61] Grossman E, Joachimski M: Oxygen isotope stratigraphy, Geologic Time Scale 2020: Elsevier, 2020: 279-307.

[62] Zheng Liduan. Environmental changes and ecological responses in the Late Neogene recorded by limnological geological lipids in Zhaotong Basin, Yunnan Province [D]. 2020.

[63] Xue Jiantao. Distribution characteristics and paleoenvironmental significance of wetland sedimentary lipids [D]. China University of Geosciences, 2018.

[64] Zheng L, Huang X J O G. Occurrence of a tetraaromatic hopane in the late Holocene peat deposit, central China[J], 2017.

[65] Huiling S, James B, Osamu S, et al. Mid- to- late Holocene hydroclimatic changes on the Chinese Loess Plateau: evidence from n-alkanes from the sediments of Tianchi Lake[J], 2018, 60.

[66] Liu J, An Z J E-S R. Leaf wax n-alkane carbon isotope values vary among major terrestrial plant groups: Different responses to precipitation amount and temperature, and implications for paleoenvironmental reconstruction[J], 2020, 202: 103081.

[67] Zhao Xiulan, Zhao Chuanben, Guan Xueting, et al. Quantitative interpretation of Tertiary paleoclimate in China using palynological data. Acta Petrolei Sinica[J], 1992(02): 215-225.

[68] Zhong Xiaochun, Zhao Chuanben, Yang Shizhong, et al. Jurassic (ii) Paleoenvironment and oil and gas in Northern China [M]. Jurassic (II) Paleoenvironment and oil and gas in Northern China, 2003.

[69] Ke Xue, Tang Tingting, Zhang Zongyan, et al. Quaternary palynological association, paleoclimate evolution sequence and regional correlation in Hengsha Island, Shanghai. Earth Science[J], 2024, 49(10): 3629-3646.

[70] Chen Jinxia, Shi Xuefa, Qiao Shuqing. Holocene palynological sequence and paleoenvironmental evolution in Bohai Sea. Journal of Oceanography[J], 2012, 34(03): 99-105.

[71] Wen R L, Xiao J L, Chang Z G, et al. Palynological records of Holocene vegetation and climate change in Hulun Lake region [J], 2010, 30(6): 1105-1115.

[72] Wei Lijie, Li Zhenhong, Li Mingtao, et al. Palynological records of the middle and late late Pleistocene in Qingshuihe Basin, Ningxia and their paleoclimatic significance [J], 2023, 29(5): 662-673.

[73] Chen Z, Wang X, Hu J, et al. Structure of the carbon isotope excursion in a high-resolution lacustrine Paleocene–Eocene Thermal Maximum record from central China[J], 2014.

[74] Chen Zuoling. Research progress on carbon cycle of Paleocene-Eocene extreme thermal events. Chinese Science Bulletin[J], 2022, 67(15): 1704-1714.

[75] Gutjahr M, Ridgwell A, Sexton P F, et al. Very large release of mostly volcanic carbon during the Palaeocene-Eocene Thermal Maximum[J], 2017.

[76] Jin S, Kemp D B, Jolley D W, et al. Large-scale, astronomically paced sediment input to the North Sea Basin during the Paleocene Eocene Thermal Maximum[J], 2022, 579: 117340-.

[77] Chen Z, Ding Z, Yang S, et al. Increased precipitation and weathering across the Paleocene-Eocene Thermal Maximum in central China[J], 2016, 17(6).

[78] Zhu Z, Liu Y, Kuang H, et al. Altered fluvial patterns in North China indicate rapid climate change linked to the Permian-Triassic mass extinction[J], 2019, 9(1): 16818.

[79] Pagani M, Pedentchouk N, Huber M, et al. Arctic hydrology during global warming at the Palaeocene/Eocene thermal maximum[J], 2006, 442(7103): 671-675.

[80] Evidence for weathering and volcanism during the PETM from Arctic Ocean and Peri-Tethys osmium isotope records. Palaeogeography Palaeoclimatology Palaeoecology[J], 2015, 438: 300-307.

[81] Kraus M J, Riggins S J P P P. Transient drying during the Paleocene–Eocene Thermal Maximum (PETM): Analysis of paleosols in the bighorn basin, Wyoming[J], 2007, 245(3-4): 444-461.

[82] Handley L, O'halloran A, Pearson P N, et al. Changes in the hydrological cycle in tropical East Africa during the Paleocene–Eocene Thermal Maximum[J], 2012, 329: 10-21.

[83] Schmitz B, Pujalte V J G. Sea-level, humidity, and land-erosion records across the initial Eocene thermal maximum from a continental-marine transect in northern Spain[J], 2003, 31(8): 689-692.

[84] Rapid Acidification of the Ocean During the Paleocean-Eocene Thermal Maximum. Science[J], 2005.

[85] Zeebe R E, Lourens L J J S. Solar System chaos and the Paleocene–Eocene boundary age constrained by geology and astronomy[J], 2019, 365(6456): 926-929.

[86] Yue Chaosheng, Chen Jitao, Yang Wenli, et al. Sedimentary response to the late Pennsylvania Subera warming event compared with the global. Acta Sedimentologica Sinica [J]: 1-19.

[87] Gong Enpu, Huang Wentao, Guan Changqing, et al. Coupling relationship between Carboniferous reef and late Paleozoic ice age. Acta Geologica Sinica[J], 2021, 95(06): 1671-1692.

[88] Ahern J P, Fielding C R J J O S R. Onset of the Late Paleozoic glacioeustatic signal: a stratigraphic record from the paleotropical, oil-shale-bearing Big Snowy Trough of Central Montana, USA[J], 2019, 89(8): 761-783.

[89] Huang W, Maillet M, Zhang Y, et al. The onset of the major glaciation of the LPIA: record from South China[J], 2020, 109: 281-300.

[90] Yao L, Qie W, Luo G, et al. The TICE event: Perturbation of carbon–nitrogen cycles during the mid-Tournaisian (Early Carboniferous) greenhouse–icehouse transition[J], 2015, 401: 1-14.

[91] Buggisch W, Joachimski M M, Sevastopulo G, et al. Mississippian δ~(13)C_(carb) and conodont apatite δ~(18)O records — Their relation to the Late Palaeozoic Glaciation[J], 2008, 268(3-4): 273-292.

[92] Fielding C R, Frank T D, Birgenheier L P, et al. Stratigraphic imprint of the Late Palaeozoic Ice Age in eastern Australia: a record of alternating glacial and nonglacial climate regime[J], 2008(1).

[93] Soreghan G S, Soreghan M J, Heavens N G J G. Explosive volcanism as a key driver of the late Paleozoic ice age[J], 2019, 47(7): 600-604.

[94] Montañez I P. Current synthesis of the penultimate icehouse and its imprint on the Upper Devonian through Permian stratigraphic record[J], 2022.

[95] Haq B U, Schutter S R J S. A chronology of Paleozoic sea-level changes[J], 2008, 322(5898): 64-68.

[96] Yu W, Algeo T J, Yan J, et al. Climatic and hydrologic controls on upper Paleozoic bauxite deposits in South China[J], 2019, 189: 159-176.

[97] Bishop J W, Monta?Ez I P, Gulbranson E L, et al. The onset of mid-Carboniferous glacio-eustasy: Sedimentologic and diagenetic constraints, Arrow Canyon, Nevada[J], 2009, 276(1-4): 217-243.

[98] Tabor N J, Poulsen C J J P, Palaeoclimatology, Palaeoecology. Palaeoclimate across the Late Pennsylvanian–Early Permian tropical palaeolatitudes: a review of climate indicators, their distribution, and relation to palaeophysiographic climate factors[J], 2008, 268(3-4): 293-310.

[99] Zhang P, Lu J, Yang M, et al. Low-latitude climate change linked to high-latitude glaciation during the Late Paleozoic Ice Age: evidence from the terrigenous detrital kaolinite[J], 2021.

[100] Gao B, Xin H, Huang X, et al. A record of enhanced water cycle in the late Paleozoic icehouse[J], 2022, 218: 103957.

[101] A W Y, C T J a a B, A J Y, et al. Climatic and hydrologic controls on upper Paleozoic bauxite deposits in South China[J], 2019, 189: 159-176.